

# *Allium cepa* L. Peel Extract Mediated Synthesis of Magnetite (Fe<sub>3</sub>O<sub>4</sub>) Nanoparticles: Application to the Removal of Phosphorus from Dam Water

Naminata Sangaré Soumahoro<sup>1</sup>, N'guessan Louis Berenger Kouassi<sup>2\*</sup>, Koffi Martin N'Goran<sup>3</sup>, Tchimou Julien Aymard Edi<sup>2</sup>, Albert Trokourey<sup>1</sup>

<sup>1</sup>Laboratory of Constitution and Reaction of Matter, University of Félix Houphouët Boigny, Abidjan, Côte d'Ivoire

<sup>2</sup>Laboratory of Chemistry, Departement of Mathematics, Physics and Chemistry, University of Peleforo Gon Coulibaly, Korhogo, Côte d'Ivoire

<sup>3</sup>Training Research Unit of Marine Sciences, Polytechnic University of San-Pedro, San-Pedro, Côte d'Ivoire

Email: \*berengerkouassi79@gmail.com

**How to cite this paper:** Soumahoro, N.S., Kouassi, N.L.B., N'Goran, K.M., Edi, T.J.A. and Trokourey, A. (2024) *Allium cepa* L. Peel Extract Mediated Synthesis of Magnetite (Fe<sub>3</sub>O<sub>4</sub>) Nanoparticles: Application to the Removal of Phosphorus from Dam Water. *Journal of Materials Science and Chemical Engineering*, 12, 18-32.

<https://doi.org/10.4236/msce.2024.1212002>

**Received:** August 27, 2024

**Accepted:** December 2, 2024

**Published:** December 5, 2024

Copyright © 2024 by author(s) and Scientific Research Publishing Inc. This work is licensed under the Creative Commons Attribution International License (CC BY 4.0).

<http://creativecommons.org/licenses/by/4.0/>



Open Access

## Abstract

Water eutrophication is generally caused by the phosphorus excessive concentration. This phenomenon may affect the water quality. Hence, phosphorus removal from dam water which is affected by agricultural activities is not well known. The present work aimed to remove phosphorus from water using green Fe<sub>3</sub>O<sub>4</sub> nanoparticles. Green iron oxide nanoparticles were prepared using the white and purple onion peels extracts. The stable iron oxide was selected using the antioxidant activity against 1,1-Diphenyl-2-Picrylhydrazyl. The SEM, XRD and FTIR analysis were used to characterize the nanoparticles. Phosphorus adsorption experiments were done in aqueous and real water solutions. The results showed that green iron oxide mediated by purple onion peels extracts possessed better antioxidant activities. The green magnetite (Fe<sub>3</sub>O<sub>4</sub>) nanoparticles obtained with the purple onion peels extracts have an average size of 15.81 nm and their surface were covered by phytochemicals compounds. In aqueous media, the optimum initial concentration of phosphate was 10 mg/L with a maximum adsorption percentage of 92%. The phosphate adsorption in aqueous solution by Fe<sub>3</sub>O<sub>4</sub> was well described by the Freundlich model. The maximum adsorption capacity was 32.05 mg/g. In addition, the results also revealed that the maximum adsorption percentage of phosphorus in the dam water was 50.13%. Green Fe<sub>3</sub>O<sub>4</sub> is therefore a good agent for removing phosphorus from polluted dam water.

## Keywords

Green Synthesis, Onion Peels, Iron Oxide, Adsorption, Phosphorus

## 1. Introduction

The eutrophication of water which generally manifests through the proliferations of micro and/or macro algae, has become a major concern [1]. This phenomenon can negatively affect the water quality and can lead, for example, to the death of fish [2]. Eutrophication of water is generally linked to excess phosphorus [3]. Important amounts of phosphorus are discharged into the aquatic environment by human activities such as agricultural practices [2]. Indeed, to increase their production, farmers use pesticides and phosphate fertilizers. In addition, phosphorus is a nonrenewable resource and in a growing world, securing sufficient phosphorus will be important to avoid its depletion. Therefore, phosphorus recovery from polluted waters is very important.

Many techniques including filtration, electrocoagulation, reverse osmosis, oxidation, and adsorption have been developed to remove phosphorus from polluted waters [4]-[8]. Due to its low cost, the adsorption technique is frequently used. The adsorption technique uses many adsorbents such as nanoparticles which are defined as materials having size between 1 and 100 nm [9]. The nanoparticles are used in many fields including medicine, cosmetics, energy, agriculture, and water treatment [10]. Chemical and physical methods such as sol-gel transition, chemical deposit in steam phase, mechanical milling, thermal decomposition and ablation laser are commonly used to synthesize the nanoparticles [11] [12]. These physico-chemical methods are costly and sometimes use toxic substances. These problems have been the subject of the development of environmentally friendly alternatives [13]-[16].

Green synthesis is advantageous because it uses substances containing phytochemicals compounds such as polyphenols, flavonoids, coumarins, tannins, phenolic acids, alkaloids, which act as reducing and stabilizing agents [17] [18]. The plants, fruit peels, and algae, extracts are among the ecological substances used in green synthesis [17]. Among the fruit peels are those of onion. The onion is consumed abundantly by the populations. However, the onion peels are released into the environment. In developing countries, the onion peels wastes cause serious disposal problems and air pollution resulting from open burning. Those low cost waste products are unused resources that can be valorized in water treatment field to reduce the environmental pollution. Hence, several authors have synthesized nanomaterials of Ag [19] [20], Fe<sub>2</sub>O<sub>3</sub> [21], Au [22], ZnO [23], and NiO [24] via onion peel extracts. As for magnetite, its ecological synthesis focused on the use of plants extracts [25]-[28]. Therefore, green synthesis of magnetite using onion peels extracts is not well known.

Due to their good magnetic properties allowing their easy separation in solution, Fe<sub>3</sub>O<sub>4</sub> nanoparticles are increasingly used to remove pollutants from wastewater [29]. Also, these nanomaterials exhibited good adsorption capacities toward trace metals, dyes and phosphorus [30]-[33]. However, studies on phosphorus removal from real wastewaters using magnetite synthesized using onion peels extracts are limited.

The aim of this study is to remove phosphorus from real polluted water using

the adsorption technique. For this purpose, green iron oxide nanoparticles were synthesized and characterized. The phosphorus adsorption isotherm was studied in aqueous media. Lastly, the effect of the mass of green iron oxide on phosphorus adsorption in dam water was investigated.

## 2. Materials and Methods

### 2.1 Preparation of the Extract

The *Allium cepa* L. peels (purple and white) were collected in the Korhogo big market. After washing several time with distilled water, the peels were dried at 30 °C in the oven during 24 h before ground and sieved. The different peel extracts were prepared by modifying the Ruiz-Baltazar *et al.* [34] method. This modified protocol is described as follow: about 20 g of purple or white onion peels were added to 100 mL of Milli Q water, and the mixture was agitated and heated during 30 min at 80 °C. After that, the solution was filtered and the obtained extract was used for experiments.

### 2.2. Green Iron Oxide Synthesis

To synthesize the green iron oxide particles, 3.475 g of  $\text{FeSO}_4 \cdot 7\text{H}_2\text{O}$  and 6.755 g of  $\text{FeCl}_3 \cdot 6\text{H}_2\text{O}$  (1/2 molar ratio) were dissolved in 125 mL of Milli Q water. A volume of 20 mL of purple or white onion peels extract was added to the solution of ( $\text{Fe}^{2+} + \text{Fe}^{3+}$ ) and the mixture was stirred at 80 °C during five minutes. The pH of the obtained mixture was adjusted between 10 and 11 using sodium hydroxide NaOH (1 M) solution [15]. The product was then separated by centrifugation and washed several time with Milli Q water after drying at 60 °C for 24 h in an oven. The green iron oxides obtained with purple, and white onion peels were denoted as PPFEO and WFeO, respectively.

### 2.3. Evaluation of the PPFEO and WFeO Antioxidant Activities

The stable radical 1,1-Diphenyl-2-Picrylhydrazyl (DPPH) was used to evaluate the antioxidant properties of PPFEO and WFeO. Firstly, a solution of 0.1 mg/mL of DPPH was prepared by dissolving 14 mg of DPPH in 140 mL of DMSO. Then, after preparation of different concentrations (2 mg/mL, 1 mg/mL, 0.5 mg/mL, 0.25 mg/mL, 0.125 mg/mL and 0.0625 mg/mL) of PPFEO or WFeO using DMSO, 1 mL of 0.1 mg/L of DPPH was added to each concentration. The mixtures were agitated and keep in the dark at 25 °C for 30 min. A spectrophotometer JENWAY was used to measure the absorbance of the sample at 517 nm [35]. The following Equation (1) was used to calculate the free radical inhibition percentage:

$$\text{Scavenging activity (\%)} = \frac{(A_b - A_i) \times 100}{A_b} \quad (1)$$

with:

$A_b$ : absorbance of the blank (control);  $A_i$ : absorbance of the sample in the presence of PPFEO or WFeO.

## 2.4. Samples Characterization by SEM, XRD and FTIR Analysis

The field-emission gun source scanning electron microscope (FEG-SEM; JEOL/JEM-1230) and the X-ray powder diffraction (XRD) were used to know the morphology and the crystallinity of the best green iron oxide, respectively. Data of XRD patterns were given by a Bruker D8 Advance X-ray diffractometer with Cu-K $\alpha$  radiation. The functional groups present on the surface of the onion peels and green iron oxide were determined using a Fourier Transform spectrophotometer Thermo Fisher Scientific Inc. Nicolet 8700 in the range of 650 and 4000 cm<sup>-1</sup>. In this section, the samples were analyzed in the powder form.

## 2.5. Phosphorus Adsorption from Aqueous and Real Solutions

In aqueous media, the isotherm adsorption experiments were done using initial phosphate concentrations of 10 mg/L, 20 mg/L, 30 mg/L, 40 mg/L, 50 mg/L, 60 mg/L, 80 mg/L, 90 mg/L and 100 mg/L. These solutions were prepared from potassium dihydrogenophosphate KH<sub>2</sub>PO<sub>4</sub> (Panreac, purity 99%). To 20 mL of each solution, 0.1 g of iron oxide was added and the mixture was stirred for 24 h. To test the adsorption capacity of green iron oxide in real solution, the Korhogo biggest dam water was collected. Korhogo is the biggest town in the northern Côte d'Ivoire. The agricultural activities using food crops were developed in this city, especially around the dam. Different amounts of iron oxide (0.05 g, 0.1 g, 0.2 g and 0.4 g) were added to 20 mL of the dam water and the suspensions were agitated for 24 h. After agitation, all suspensions were centrifuged at 5000 rpm for 10 min and the supernatants were analyzed at 700 nm using a spectrophotometer HACH DR6000 to determine the phosphorus content using the Murphy and Riley method [36]. The amounts and percentages of phosphorus after adsorption were calculated using the Equations (2) and (3), respectively.

$$q_e = \frac{(C_0 - C_e) \times V}{m} \quad (2)$$

$$\% ADS = \frac{(C_0 - C_e) \times 100}{C_0} \quad (3)$$

In the Equations (2) and (3),  $C_0$  (mg/L),  $C_e$  (mg/L),  $m$  (g),  $V$  (L) are the initial concentration, equilibrium concentration, the mass of the adsorbent and the volume of the solution, respectively.

Phosphorus adsorption data in aqueous solution were fitted using the nonlinear forms of Langmuir [37] and Freundlich [38] models indicated by the Equations (4) and (5), respectively

$$q_e = \frac{Q_{\max} \times K_L \times C_e}{1 + K_L \times C_e} \quad (4)$$

$$q_e = K_F \times C_e^{1/n} \quad (5)$$

$C_e$  (mg/L) is the equilibrium concentration of phosphorus;

$q_e$  (mg/g) is the phosphorus amount adsorbed at equilibrium;

$K_L$  and  $K_F$  are the Langmuir and Freundlich constants, respectively;

$Q_{\max}$  (mg/g) is the maximum amount adsorbed;

$n$  is the Freundlich model exponent.

An error analysis based on the sum of squares ( $SSE$ ) and chi-square ( $\chi^2$ ) has been carried out in order to find the best non-linear model.

$$SSE = \sum_{i=1}^n (q_{e\ exp} - q_{e\ cal})^2 \quad (6)$$

$$\chi^2 = \sum_{i=1}^n \frac{(q_{e\ exp} - q_{e\ cal})^2}{q_{e\ cal}} \quad (7)$$

where  $q_{e\ cal}$  and  $q_{e\ exp}$  are predicted and experimental adsorption data, respectively.

### 3. Results and Discussion

#### 3.1. Antioxidant Activity

**Figure 1** indicates the percentages of DPPH inhibition by iron oxide particles synthesized with white onion (WFeO) and with purple onion (PPFeO). The scavenging activity of DPPH varied from 5.89% to 24.89% for iron oxide PPFeO. Whereas, that for iron oxide WFeO increased from 1.84% to 18.01%. Data obtained with PPFeO were higher than those obtained with WFeO, showing that the PPFeO particles possess good antioxidant properties than WFeO particles. That can be explained by the fact that there are more phytochemicals present on the PPFeO surface [15]. According to Mondal *et al.* [17], phytochemicals compounds present in plants, peels and fruits enhance the stability of nanoparticles. Therefore, the iron oxide PPFeO particles are most stable than iron oxide WFeO particles. Thus, PPFeO particles seem to be the most appropriate for various applications. Authors such as Kouassi *et al.* [15] and Kumar *et al.* [39] showed remarkable antioxidant activities for iron oxide particles synthesized with grapefruit peels extract and citrus peels extract, respectively. These findings corroborate ours.

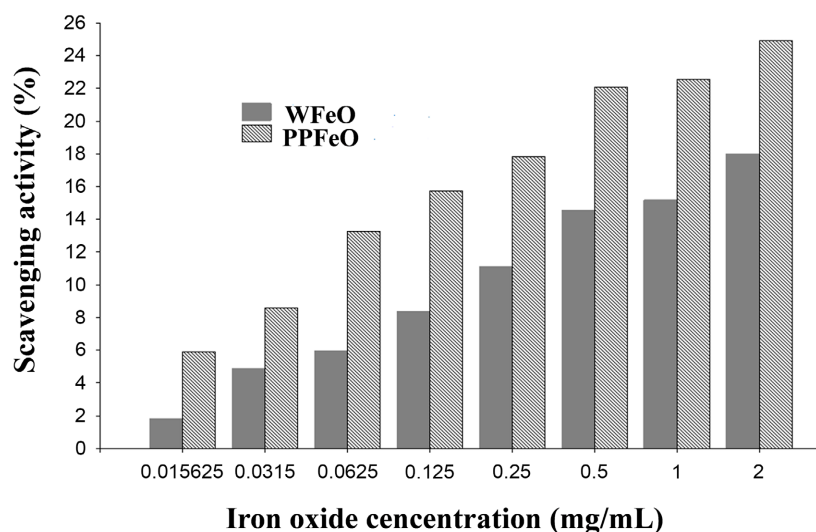


**Figure 1.** Antioxidant activity of WFeO and PPFeO against DPPH.

### 3.2. SEM, XRD and FTIR Analysis of Iron Oxide PPF<sub>FeO</sub>

The morphology of PPF<sub>FeO</sub> nanoparticles is given by **Figure 2**. The results of SEM image of PPF<sub>FeO</sub> particles showed semi-spherical with agglomerates. The phytochemicals from onion peels present on the surface of PPF<sub>FeO</sub> and the magnetic interaction due to iron oxide particles can explain the agglomeration [15] [34].

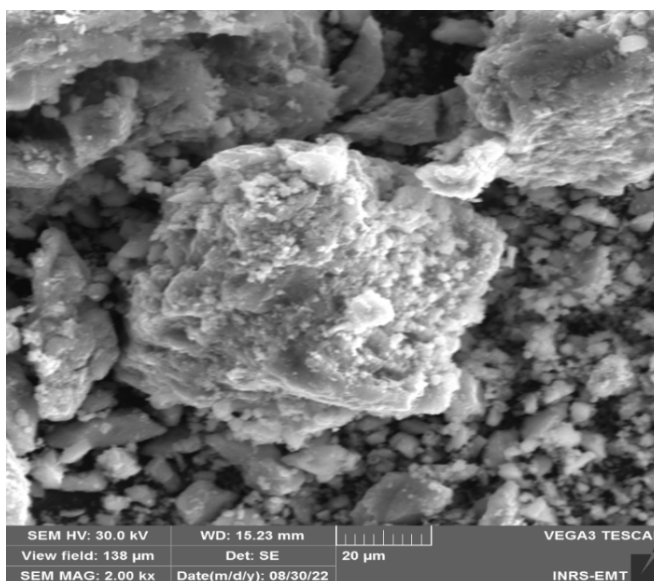


**Figure 2.** SEM image of PPF<sub>FeO</sub>.

**Figure 3** indicates XRD data for PPF<sub>FeO</sub> particles. Different diffraction peaks were observed at 18.27° $2\theta$ , 21.16° $2\theta$ , 30.11° $2\theta$ , 30.21° $2\theta$ , 35.42° $2\theta$ , 43.12° $2\theta$ , 47.16° $2\theta$ , 57.09° $2\theta$ , 62.82° $2\theta$ , 66.02° $2\theta$ , 73.91° $2\theta$ , 75.22° $2\theta$ , and 82.95° $2\theta$  which correspond to the index (011), (002), (112), (200), (121), (004), (123), (204), (321), (400), (411), (143), (422), and (226), respectively. According to the reference data of JCPDS 39-1346 (Joint Committee on Powder Diffraction Standards), our findings show the formation of magnetite (Fe<sub>3</sub>O<sub>4</sub>). The intense peaks observed at 30.21° $2\theta$  (index 200) and 35.42° $2\theta$  (index 121) reveal the crystalline nature of Fe<sub>3</sub>O<sub>4</sub> particles [40]. The average size of the green Fe<sub>3</sub>O<sub>4</sub> particles calculated using the Debye-Scherrer relationship was 15.81 nm, that confirms their nanometric nature. According to Strambeanu *et al.* [9] the size of the nanoparticles vary between 1 and 100 nm. Our results corroborate those of Bouafia *et al.* [25] and Stan *et al.* [41]. Bouafia *et al.* [25] and Stan *et al.* [41] obtained green Fe<sub>3</sub>O<sub>4</sub> nanoparticles with an average sizes of 19 nm and 8 nm using Atelesia leaves and lemon peels, respectively.

**Figure 4** shows the results of FTIR for purple onion peel (a) and purple peel iron oxide Fe<sub>3</sub>O<sub>4</sub> (b). Specific peaks for the purple onion peels were observed at 1010 cm<sup>-1</sup>, 1310 cm<sup>-1</sup>, 2200 cm<sup>-1</sup> and 2900 cm<sup>-1</sup>, and those for Fe<sub>3</sub>O<sub>4</sub> were observed at 813 cm<sup>-1</sup>, 1110 cm<sup>-1</sup>, 2020 cm<sup>-1</sup> and 2580 cm<sup>-1</sup>. Similar peaks to the two compounds were obtained at 1420 cm<sup>-1</sup>, 1620 cm<sup>-1</sup>, 2200 cm<sup>-1</sup> and 3320 cm<sup>-1</sup>. The strips obtained 3320 cm<sup>-1</sup> are attributed to the O-H stretching of the phenolic or

alcoholic groups of flavonoids [11] [42]. At  $3320\text{ cm}^{-1}$ , the band observed with  $\text{Fe}_3\text{O}_4$  spectrum is broader than that with onion peels. This is explained by the interaction between onion peel extracts and iron solutions [42]. The Peaks obtained at  $1620\text{ cm}^{-1}$  were assigned to C=O vibrations of aldehydes and ketones, revealing the phenolic acids and terpenoids [39]. In addition, the common peak at  $1420\text{ cm}^{-1}$  indicates the presence of aromatic compounds such as polysaccharides [34]. The peaks obtained at  $2900\text{ cm}^{-1}$  and  $1310\text{ cm}^{-1}$  on the yellow onion peels' spectrum were associated to C-H bond of the methyl group and C-O of acidic groups, respectively [42] [43]. The observed peaks at  $1010\text{ cm}^{-1}$  and  $1110\text{ cm}^{-1}$ , with purple onion peels and  $\text{Fe}_3\text{O}_4$ , respectively, are associated to the flavonoids' aliphatic amine group [34]. Thus, flavones and flavonols could be involved in the reduction of iron ions and consequently in the formation of iron oxide ( $\text{Fe}_3\text{O}_4$ ). Flores-Cano *et al.* [44] reported the range of  $900 - 410\text{ cm}^{-1}$  as the Fe-O bonding characteristic region. Therefore, the peak obtained at  $813\text{ cm}^{-1}$  with the iron oxide ( $\text{Fe}_3\text{O}_4$ ) spectrum, indicates the presence of the Fe-O bond of  $\text{Fe}_3\text{O}_4$ . In this study, data obtained with FTIR corroborate those of XRD.

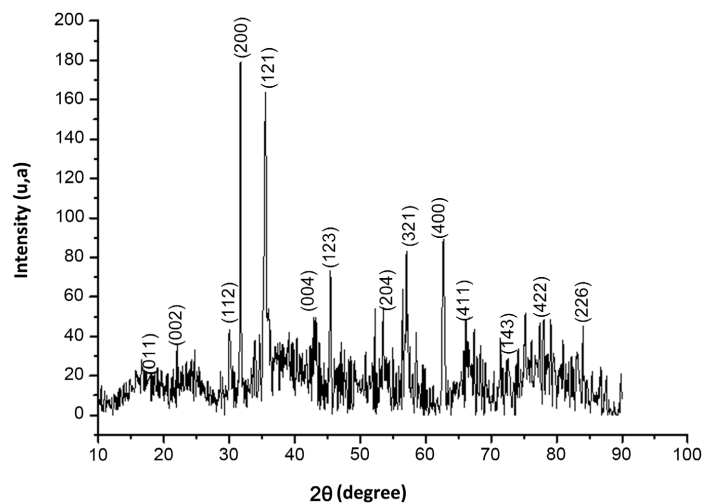


**Figure 3.** XRD patterns of PPFEO.

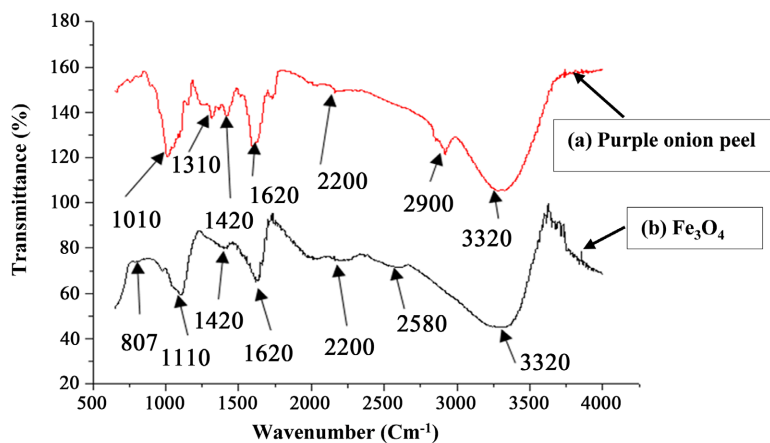


**Figure 4.** FTIR spectrum of purple onion peels (a) and PPFEO ( $\text{Fe}_3\text{O}_4$ ) nanoparticles (b).

### 3.3. Adsorption of Phosphorus in Aqueous and Real Solutions

#### 3.3.1. Adsorption in Aqueous Solution

**Figure 5(a)** shows that phosphate adsorption percentage decreased from 92% to 66.2% when the initial concentration of phosphate increased from 10 mg/L to 100 mg/L. The reduction of the phosphate adsorption is explained by the saturation of the adsorption sites of iron oxides  $\text{Fe}_3\text{O}_4$ .

The amount of phosphate adsorbed increased with the increase in its equilibrium concentration (**Figure 5(b)**), indicating a good adsorption capacity of  $\text{Fe}_3\text{O}_4$  towards phosphorus.

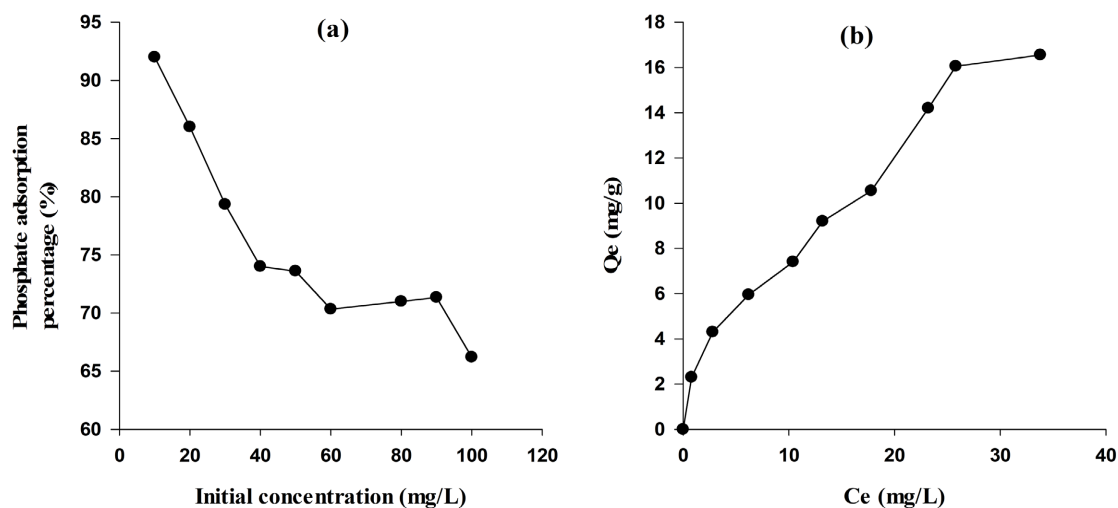


**Figure 5.** Effect of initial concentration on phosphate adsorption (a) and adsorption isotherm of phosphate (b).

Phosphate adsorption data were fitted using Langmuir and Freundlich non-linear models. The results are given by **Figure 6** and summarize in **Table 1**. It has been observed that, the values of  $\chi^2$  et SSE obtained with the Langmuir model ( $\chi^2 = 4.29$ , SSE = 9.80) were higher than those of Freundlich ( $\chi^2 = 0.79$ , SSE = 5.99).

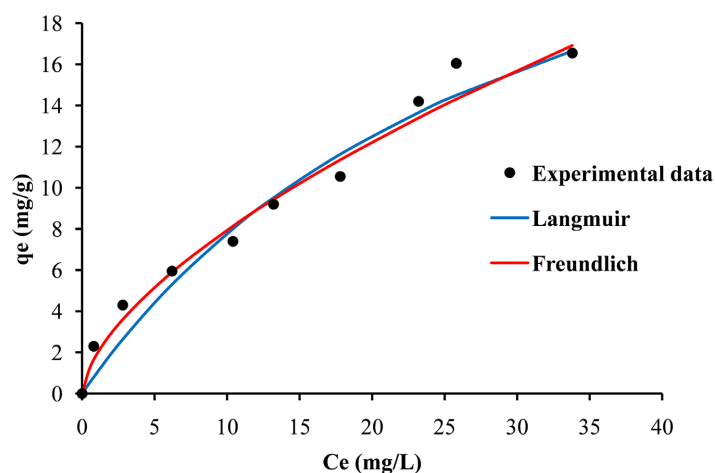


**Figure 6.** Nonlinear Freundlich isotherm and nonlinear Langmuir isotherm for phosphate adsorption.

**Table 1.** Parameters of langmiur and freundlich models.

Models	Parameters	Values
Langmuir	$Q_{\max}$ (mg/g)	32.05
	$K_L$	0.032
	$R^2$	0.967
	$\chi^2$	4.29
	$SSE$	9.80
Freundlich	$K_F$	1.90
	$n$	1.61
	$R^2$	0.972
	$\chi^2$	0.79
	$SSE$	5.99

$K_L$  and  $K_F$  are the Langmuir and Freundlich constants, respectively.  $R^2$  is the coefficient of determination.

It has been reported that, when the error is smaller, the model is better [15] [45]. Therefore, phosphate adsorption in aqueous solution by  $Fe_3O_4$  was well described by the Freundlich model. These finding are in agreement with those of Fu *et al.* [32]. Indeed, these authors reported that phosphorus adsorption in aqueous solution by  $Fe_3O_4$  synthesized under an  $N_2$  atmosphere was well described by Freundlich model.

**Table 2** indicates the maximum adsorption capacity ( $Q_m$ ) of phosphate obtained in this study and thoses from the literature. Data from the present study (32.05 mg/g) was lower than those reported by Qingliang *et al.* [1], Han *et al.* [5], Li *et al.* [46], and Yan *et al.* [47]. On the contrary, our data was higher than those obtained by Cao *et al.* [48], Afridi *et al.* [4], and Funes *et al.* [33]. These low values compared to our data would be due to the nature of the biological material, and the nature of the solvent used to prepare the extract. Indeed, green  $Fe_3O_4$  nanoparticles were synthesized by Cao *et al.* [48], and Afridi *et al.* [4] using *eucalyptus* leaf extract, and bovine serum albumin, respectively.

**Table 2.** Comparison of adsorption capacities of different adsorbents for phosphate removal.

Adsorbents	Adsorption capacity Qmax (mg/g)	References
$Fe_3O_4$ synthesized with purple onion peels	32.05	Present study
$\gamma-Al_2O_3/Fe_3O_4$ biochar	181.4	[1]
$Fe_3O_4$ synthesized with bovine serum albumin	20.7	[4]
Chitosan@ $Fe_3O_4$	98	[5]
$Fe_3O_4$ @Chitosan	48.2	[32]

## Continued

Fe <sub>3</sub> O <sub>4</sub> synthesized by solvothermal method	2.27	[33]
MgO@Fe <sub>3</sub> O <sub>4</sub> @SiO <sub>2</sub>	223.6	[46]
Fe <sub>3</sub> O <sub>4</sub> @LDH (Layered double hydroxides)	36.9	[47]
Fe <sub>3</sub> O <sub>4</sub> synthesized with <i>Eucalyptus</i> leaf extract	18.7	[48]

### 3.3.2. Adsorption in Real Solution

In real solution (dam water), the adsorption percentage of phosphate varied between 32.89% and 50.13% (Table 3). The maximum adsorption percentage (50.13%) was obtained with Fe<sub>3</sub>O<sub>4</sub> mass of 0.1 g. Therefore, green Fe<sub>3</sub>O<sub>4</sub> may be proposed to remove phosphate from polluted dam water. Data obtained with the real solution were lower than those for the aqueous solution. This is due to the competition between phosphates and the other pollutants present in the dam water [45] [49].

**Table 3.** Dam water treatment.

Mass (g)	Before adsorption (mg/L)	After adsorption (mg/L)	Adsorption percentage (%)
0.05	15.2	10.2	32.89
0.1	15.2	7.58	50.13
0.2	15.2	9.20	39.47
0.4	15.2	9.20	39.47

## 4. Conclusion

The present work investigated the ability of green magnetite synthesized using onion peels extracts to remove phosphorus from polluted water. The results showed that green iron oxide mediated by purple onion peels extracts possesses higher antioxidant activity (5.89% to 24.89%), than iron oxide prepared with white onion peels extracts (1.84% to 18.01%), indicating higher stability for iron oxide synthesized with purple onion peels extracts. XRD data indicated the formation of magnetite (Fe<sub>3</sub>O<sub>4</sub>) nanoparticles with an average size of 15.81 nm. The surface of green Fe<sub>3</sub>O<sub>4</sub> was covered by phytochemicals compounds present in the purple onion peels indicated by FTIR data. The results of adsorption experiments in aqueous media showed that the phosphorus initial concentration affected phosphate adsorption with a maximum adsorption percentage of 92% for initial concentration of 10 mol/L. The phosphate adsorption in aqueous solution by Fe<sub>3</sub>O<sub>4</sub> was well described by the Freundlich model. With the dam water, the maximum adsorption percentage of phosphate was 50.13%. Therefore, green Fe<sub>3</sub>O<sub>4</sub> is a good candidate to remove phosphorus from polluted dam water.

## Availability of Data

The data used in this study are available from the corresponding author on reasonable request.

## Author Contributions

**Naminata Sangaré Soumahoro:** Conceptualization, data curation, formal analysis, investigation, methodology, validation, writing original draft, writing-review draft, and editing. **N'guessan Louis Berenger Kouassi:** Conceptualization, data curation, formal analysis, investigation, methodology, validation, writing-original draft, writing-review draft, and editing. **Koffi Martin N'Goran:** Conceptualization, data curation, formal analysis, investigation, methodology, validation, writing-original draft, writing-review draft, and editing. **Edi Tchimou Julien Aymard:** Conceptualization, data curation, formal analysis, investigation, methodology, validation, writingoriginal draft, writing-review draft, and editing. **Albert Trokourey:** Conceptualization, data curation, formal analysis, investigation, methodology, supervision, validation, writing-original draft, writing-review draft, and editing.

## Acknowledgements

The authors express their gratitude to the President of Peleforo GON COULIBALY University, Korhogo for facilitating the experiments in the laboratory. Special thanks to the reviewers for helping to improve this work.

## Conflicts of Interest

No conflict of interest exists among the authors.

## References

- [1] Cui, Q., Xu, J., Wang, W., Tan, L., Cui, Y., Wang, T., *et al.* (2020) Phosphorus Recovery by Core-Shell  $\gamma$ -Al<sub>2</sub>O<sub>3</sub>/Fe<sub>3</sub>O<sub>4</sub> Biochar Composite from Aqueous Phosphate Solutions. *Science of the Total Environment*, **729**, Article ID: 138892. <https://doi.org/10.1016/j.scitotenv.2020.138892>
- [2] Akinnawo, S.O. (2023) Eutrophication: Causes, Consequences, Physical, Chemical and Biological Techniques for Mitigation Strategies. *Environmental Challenges*, **12**, Article ID: 100733. <https://doi.org/10.1016/j.envc.2023.100733>
- [3] Dupas, R., Delmas, M., Dorioz, J., Garnier, J., Moatar, F. and Gascuel-Oudou, C. (2015) Assessing the Impact of Agricultural Pressures on N and P Loads and Eutrophication Risk. *Ecological Indicators*, **48**, 396-407. <https://doi.org/10.1016/j.ecolind.2014.08.007>
- [4] Afridi, M.N., Lee, W. and Kim, J. (2020) Application of Synthesized Bovine Serum Albumin-Magnetic Iron Oxide for Phosphate Recovery. *Journal of Industrial and Engineering Chemistry*, **86**, 113-122. <https://doi.org/10.1016/j.jiec.2020.02.018>
- [5] Han, Y., Ma, Z., Cong, H., Wang, Q. and Wang, X. (2022) Surface Chitosan-Coated Fe<sub>3</sub>O<sub>4</sub> Immobilized Lignin for Adsorbed Phosphate Radicals in Solution. *Biochemical Engineering Journal*, **187**, Article ID: 108662. <https://doi.org/10.1016/j.bej.2022.108662>
- [6] Li, T., Dong, W., Zhang, Q., Xing, D., Ai, W. and Liu, T. (2020) Phosphate Removal

- from Industrial Wastewater through *In-Situ* Fe<sup>2+</sup> Oxidation Induced Homogenous Precipitation: Different Oxidation Approaches at Wide-Ranged pH. *Journal of Environmental Management*, **255**, Article ID: 109849. <https://doi.org/10.1016/j.jenvman.2019.109849>
- [7] Liu, D. and Zhou, S. (2021) Application of Chemical Coagulation to Phosphorus Removal from Glyphosate Wastewater. *International Journal of Environmental Science and Technology*, **19**, 2345-2352. <https://doi.org/10.1007/s13762-021-03164-x>
- [8] Ramashree, T., Rahman, S.S.A., Pasupathi, S., Asaithambi, K., Mathivanan, M. and Karuppiah, S. (2024) Valorization of Spent Aureobasidium Pullulans for the Removal of Toxic Pollutant in Wastewater Treatment. *Kuwait Journal of Science*, **51**, Article ID: 100123. <https://doi.org/10.1016/j.kjs.2023.08.006>
- [9] Strambeanu, N., Demetrovici, L., Dragos, D. and Lungu, M. (2014) Nanoparticles: Definition, Classification and General Physical Properties. In: Lungu, M., Neculae, A., Bunoiu, M., Biris, C., *et al.*, Eds., *Nanoparticles' Promises and Risks*, Springer International Publishing, 3-8. [https://doi.org/10.1007/978-3-319-11728-7\\_1](https://doi.org/10.1007/978-3-319-11728-7_1)
- [10] Karunakaran, S., Ramanujam, S. and Gurunathan, B. (2018) Green Synthesised Iron and Iron-Based Nanoparticle in Environmental and Biomedical Application: A Review. *IET Nanobiotechnology*, **12**, 1003-1008. <https://doi.org/10.1049/iet-nbt.2018.5048>
- [11] Abdullah, J.A.A., Salah Eddine, L., Abderrhmane, B., Alonso-González, M., Guerrero, A. and Romero, A. (2020) Green Synthesis and Characterization of Iron Oxide Nanoparticles by Phoenix Dactylifera Leaf Extract and Evaluation of Their Antioxidant Activity. *Sustainable Chemistry and Pharmacy*, **17**, Article ID: 100280. <https://doi.org/10.1016/j.scp.2020.100280>
- [12] Justin, C., Philip, S.A. and Samrot, A.V. (2017) Synthesis and Characterization of Superparamagnetic Iron-Oxide Nanoparticles (SPIONs) and Utilization of Spions in X-Ray Imaging. *Applied Nanoscience*, **7**, 463-475. <https://doi.org/10.1007/s13204-017-0583-x>
- [13] Gamedze, N.P., Mthiyane, D.M.N., Mavengahama, S., Singh, M. and Onwudiwe, D.C. (2023) Biosynthesis of ZnO Nanoparticles Using the Aqueous Extract of Mucuna Pruriens (Utilis): Structural Characterization, and the Anticancer and Antioxidant Activities. *Chemistry Africa*, **7**, 219-228. <https://doi.org/10.1007/s42250-023-00750-z>
- [14] Hudaya, I.R., Mukti, G.I., Kasasiah, A., Hilmi, I.L., Kristiana, R., Okselni, T., *et al.* (2023) Eco-Friendly Green Synthesis of Silver Nanoparticles Using Toona Sureni (Blume) Merr. Leaf Extract and Evaluation of Its Antibacterial Activity against Selected Clinical Isolates. *Chemistry Africa*, **7**, 1311-1321. <https://doi.org/10.1007/s42250-023-00829-7>
- [15] Kouassi, N.L.B., Diabate, D., Pohan, L.A.G., Ossonon, B.D., Blonde, L.D., Trokourey, A. (2022) Green Synthesis of Iron Oxide Nanoparticles Using Grapefruit Peel Extract: Application for Removal of Indigo Carmine Dye from Industrial Wastewater. *American Journal of Physical and Chemistry*, **11**, 110-119.
- [16] Şahin, A., Altınsoy, Ş. and Kızılbaş, K. (2024) An Approach for Cationic Dyes Removal from Wastewater: Green Synthesis of Iron Nanoparticles Using Prunus Avium Stems Extracts. *Kuwait Journal of Science*, **51**, Article ID: 100226. <https://doi.org/10.1016/j.kjs.2024.100226>
- [17] Mondal, P., Anweshan, A. and Purkait, M.K. (2020) Green Synthesis and Environmental Application of Iron-Based Nanomaterials and Nanocomposite: A Review. *Chemosphere*, **259**, Article ID: 127509. <https://doi.org/10.1016/j.chemosphere.2020.127509>

- [18] Begum, S., Sahoo, T., Swain, S., Nayak, A., Shivangi Das, S.P., Rath, S.K., *et al.* (2024) Fabrication of Iron Nanoparticles Using Different Bioactive Precursors, Their Characterization and Bioactivity Evaluation. *Sustainable Chemistry for the Environment*, **6**, Article ID: 100100. <https://doi.org/10.1016/j.scenv.2024.100100>
- [19] Santhosh, A., Theertha, V., Prakash, P. and Smitha Chandran, S. (2021) From Waste to a Value Added Product: Green Synthesis of Silver Nanoparticles from Onion Peels Together with Its Diverse Applications. *Materials Today: Proceedings*, **46**, 4460-4463. <https://doi.org/10.1016/j.matpr.2020.09.680>
- [20] Yap, Y.H., Azmi, A.A., Mohd, N.K., Yong, F.S.J., Kan, S., Thirminzir, M.Z.A., *et al.* (2020) Green Synthesis of Silver Nanoparticle Using Water Extract of Onion Peel and Application in the Acetylation Reaction. *Arabian Journal for Science and Engineering*, **45**, 4797-4807. <https://doi.org/10.1007/s13369-020-04595-3>
- [21] Abid, M.A., Abid, D.A., Aziz, W.J. and Rashid, T.M. (2021) Iron Oxide Nanoparticles Synthesized Using Garlic and Onion Peel Extracts Rapidly Degrade Methylene Blue Dye. *Physica B: Condensed Matter*, **622**, Article ID: 413277. <https://doi.org/10.1016/j.physb.2021.413277>
- [22] Patra, J.K., Kwon, Y. and Baek, K. (2016) Green Biosynthesis of Gold Nanoparticles by Onion Peel Extract: Synthesis, Characterization and Biological Activities. *Advanced Powder Technology*, **27**, 2204-2213. <https://doi.org/10.1016/j.apt.2016.08.005>
- [23] Islam, M.F., Islam, S., Miah, M.A.S., Huq, A.K.O., Saha, A.K., Mou, Z.J., *et al.* (2024) Green Synthesis of Zinc Oxide Nano Particles Using *Allium cepa* L. Waste Peel Extracts and Its Antioxidant and Antibacterial Activities. *Heliyon*, **10**, e25430. <https://doi.org/10.1016/j.heliyon.2024.e25430>
- [24] Rafique, M.A., Kiran, S., Javed, S., Ahmad, I., Yousaf, S., Iqbal, N., *et al.* (2021) Green Synthesis of Nickel Oxide Nanoparticles Using *Allium cepa* Peels for Degradation of Congo Red Direct Dye: An Environmental Remedial Approach. *Water Science and Technology*, **84**, 2793-2804. <https://doi.org/10.2166/wst.2021.237>
- [25] Bouafia, A., Laouini, S.E., Khelef, A., Tedjani, M.L. and Guemari, F. (2020) Effect of Ferric Chloride Concentration on the Type of Magnetite (Fe<sub>3</sub>O<sub>4</sub>) Nanoparticles Biosynthesized by Aqueous Leaves Extract of Artemisia and Assessment of Their Antioxidant Activities. *Journal of Cluster Science*, **32**, 1033-1041. <https://doi.org/10.1007/s10876-020-01868-7>
- [26] Devi, H.S., Boda, M.A., Shah, M.A., Parveen, S. and Wani, A.H. (2019) Green Synthesis of Iron Oxide Nanoparticles Using Platanus Orientalis Leaf Extract for Antifungal Activity. *Green Processing and Synthesis*, **8**, 38-45. <https://doi.org/10.1515/gps-2017-0145>
- [27] Nnadozie, E.C. and Ajibade, P.A. (2020) Green Synthesis and Characterization of Magnetite (Fe<sub>3</sub>O<sub>4</sub>) Nanoparticles Using Chromolaena Odorata Root Extract for Smart Nanocomposite. *Materials Letters*, **263**, Article ID: 127145. <https://doi.org/10.1016/j.matlet.2019.127145>
- [28] Ramesh, A.V., Rama Devi, D., Mohan Botsa, S. and Basavaiah, K. (2018) Facile Green Synthesis of Fe<sub>3</sub>O<sub>4</sub> Nanoparticles Using Aqueous Leaf Extract of *Zanthoxylum armatum* DC. for Efficient Adsorption of Methylene Blue. *Journal of Asian Ceramic Societies*, **6**, 145-155. <https://doi.org/10.1080/21870764.2018.1459335>
- [29] Braim, F.S., Nik Ab Razak, N.N.A., Aziz, A.A., Dheyab, M.A. and Ismael, L.Q. (2023) Rapid Green-Assisted Synthesis and Functionalization of Superparamagnetic Magnetite Nanoparticles Using Sumac Extract and Assessment of Their Cellular Toxicity, Uptake, and Anti-Metastasis Property. *Ceramics International*, **49**, 7359-7369. <https://doi.org/10.1016/j.ceramint.2022.10.207>

- [30] Chamchoy, K., Inprasit, T., Vanichvattanadecha, C., Thiangtrong, A., Anukunwithaya, P. and Pisitsak, P. (2020) The Magnetic Properties and Dye Adsorption of Sericin-Modified Magnetite Nanoparticles. *Journal of Polymers and the Environment*, **29**, 484-491. <https://doi.org/10.1007/s10924-020-01891-9>
- [31] El-Dib, F.I., Mohamed, D.E., El-Shamy, O.A.A. and Mishrif, M.R. (2020) Study the Adsorption Properties of Magnetite Nanoparticles in the Presence of Different Synthesized Surfactants for Heavy Metal Ions Removal. *Egyptian Journal of Petroleum*, **29**, 1-7. <https://doi.org/10.1016/j.ejpe.2019.08.004>
- [32] Fu, C., Tran, H.N., Chen, X. and Juang, R. (2020) Preparation of Polyaminated Fe<sub>3</sub>O<sub>4</sub>@Chitosan Core-Shell Magnetic Nanoparticles for Efficient Adsorption of Phosphate in Aqueous Solutions. *Journal of Industrial and Engineering Chemistry*, **83**, 235-246. <https://doi.org/10.1016/j.jiec.2019.11.033>
- [33] Funes, A., de Vicente, J. and de Vicente, I. (2017) Synthesis and Characterization of Magnetic Chitosan Microspheres as Low-Density and Low-Biototoxicity Adsorbents for Lake Restoration. *Chemosphere*, **171**, 571-579. <https://doi.org/10.1016/j.chemosphere.2016.12.101>
- [34] Ruíz-Baltazar, Á.d.J., Reyes-López, S.Y., Mondragón-Sánchez, M.d.L., Robles-Cortés, A.I. and Pérez, R. (2019) Eco-Friendly Synthesis of Fe<sub>3</sub>O<sub>4</sub> Nanoparticles: Evaluation of Their Catalytic Activity in Methylene Blue Degradation by Kinetic Adsorption Models. *Results in Physics*, **12**, 989-995. <https://doi.org/10.1016/j.rinp.2018.12.037>
- [35] Zeraik, M.L., Serteyn, D., Deby-Dupont, G., Wauters, J., Tits, M., Yariwake, J.H., *et al.* (2011) Evaluation of the Antioxidant Activity of Passion Fruit (*Passiflora edulis* and *Passiflora alata*) Extracts on Stimulated Neutrophils and Myeloperoxidase Activity Assays. *Food Chemistry*, **128**, 259-265. <https://doi.org/10.1016/j.foodchem.2011.03.001>
- [36] Murphy, J. and Riley, J.P. (1962) A Modified Single Solution Method for the Determination of Phosphate in Natural Waters. *Analytica Chimica Acta*, **27**, 31-36. [https://doi.org/10.1016/s0003-2670\(00\)88444-5](https://doi.org/10.1016/s0003-2670(00)88444-5)
- [37] Langmuir, I. (1918) The Adsorption of Gases on Plane Surfaces of Glass, Mica and Platinum. *Journal of the American Chemical Society*, **40**, 1361-1403. <https://doi.org/10.1021/ja02242a004>
- [38] Freundlich, H. (1907) Über die Adsorption in Lösungen. *Zeitschrift für Physikalische Chemie*, **57**, 385-470. <https://doi.org/10.1515/zpch-1907-5723>
- [39] Kumar, B., Smita, K., Galeas, S., Sharma, V., Guerrero, V.H., Debut, A., *et al.* (2020) Characterization and Application of Biosynthesized Iron Oxide Nanoparticles Using Citrus Paradisi Peel: A Sustainable Approach. *Inorganic Chemistry Communications*, **119**, Article ID: 108116. <https://doi.org/10.1016/j.inoche.2020.108116>
- [40] Bhuiyan, M.S.H., Miah, M.Y., Paul, S.C., Aka, T.D., Saha, O., Rahaman, M.M., *et al.* (2020) Green Synthesis of Iron Oxide Nanoparticle Using Carica Papaya Leaf Extract: Application for Photocatalytic Degradation of Remazol Yellow RR Dye and Antibacterial Activity. *Heliyon*, **6**, e04603. <https://doi.org/10.1016/j.heliyon.2020.e04603>
- [41] Stan, M., Lung, I., Soran, M., Leostean, C., Popa, A., Stefan, M., *et al.* (2017) Removal of Antibiotics from Aqueous Solutions by Green Synthesized Magnetite Nanoparticles with Selected Agro-Waste Extracts. *Process Safety and Environmental Protection*, **107**, 357-372. <https://doi.org/10.1016/j.psep.2017.03.003>
- [42] Kumar, B., Smita, K., Cumbal, L., Debut, A., Galeas, S. and Guerrero, V.H. (2016) Phytosynthesis and Photocatalytic Activity of Magnetite (Fe<sub>3</sub>O<sub>4</sub>) Nanoparticles Using the Andean Blackberry Leaf. *Materials Chemistry and Physics*, **179**, 310-315. <https://doi.org/10.1016/j.matchemphys.2016.05.045>

- [43] Venkateswarlu, S., Kumar, B.N., Prathima, B., SubbaRao, Y. and Jyothi, N.V.V. (2019) A Novel Green Synthesis of Fe<sub>3</sub>O<sub>4</sub> Magnetic Nanorods Using Punica Granatum Rind Extract and Its Application for Removal of Pb(II) from Aqueous Environment. *Arabian Journal of Chemistry*, **12**, 588-596. <https://doi.org/10.1016/j.arabjc.2014.09.006>
- [44] Flores-Cano, D.A., Checca-Huaman, N., Castro-Merino, I., Pinotti, C.N., Passamani, E.C., Litterst, F.J., *et al.* (2022) Progress toward Room-Temperature Synthesis and Functionalization of Iron-Oxide Nanoparticles. *International Journal of Molecular Sciences*, **23**, Article No. 8279. <https://doi.org/10.3390/ijms23158279>
- [45] Kouassi, N.L.B., N'goran, K.P.D.A., Blonde, L.D., Diabate, D. and Albert, T. (2022) Simultaneous Removal of Copper and Lead from Industrial Effluents Using Corn Cob Activated Carbon. *Chemistry Africa*, **6**, 733-745. <https://doi.org/10.1007/s42250-022-00432-2>
- [46] Li, S., Zhang, Y., Qiao, S. and Zhou, J. (2022) MgO Coated Magnetic Fe<sub>3</sub>O<sub>4</sub>@SiO<sub>2</sub> Nanoparticles with Fast and Efficient Phosphorus Removal Performance and Excellent pH Stability. *Chemosphere*, **307**, Article ID: 135972. <https://doi.org/10.1016/j.chemosphere.2022.135972>
- [47] Yan, L., Yang, K., Shan, R., Yan, T., Wei, J., Yu, S., *et al.* (2015) Kinetic, Isotherm and Thermodynamic Investigations of Phosphate Adsorption onto Core-Shell Fe<sub>3</sub>O<sub>4</sub>@LDHs Composites with Easy Magnetic Separation Assistance. *Journal of Colloid and Interface Science*, **448**, 508-516. <https://doi.org/10.1016/j.jcis.2015.02.048>
- [48] Cao, D., Jin, X., Gan, L., Wang, T. and Chen, Z. (2016) Removal of Phosphate Using Iron Oxide Nanoparticles Synthesized by Eucalyptus Leaf Extract in the Presence of CTAB Surfactant. *Chemosphere*, **159**, 23-31. <https://doi.org/10.1016/j.chemosphere.2016.05.080>
- [49] Almeida, P.V., Santos, A.F., Lopes, D.V., Gando-Ferreira, L.M. and Quina, M.J. (2020) Novel Adsorbents Based on Eggshell Functionalized with Iron Oxyhydroxide for Phosphorus Removal from Liquid Effluents. *Journal of Water Process Engineering*, **36**, Article ID: 101248. <https://doi.org/10.1016/j.jwpe.2020.101248>